Dalton Transactions

PAPER

View Article Online
View Journal | View Issue

Open Access Article. Published on 16 February 2015. Downloaded on 8/23/2022 12:27:23 PM.
This article is licensed under a Creative Commons Attribution 3.0 Unported Licence.

Cite this: *Dalton Trans.*, 2015, **44**, 6784

The titanium tris-anilide cation $[Ti(N[^tBu]Ar)_3]^+$ stabilized as its perfluoro-tetra-phenylborate salt: structural characterization and synthesis in connection with redox activity of 4,4′-bipyridine dititanium complexes†

Heather A. Spinney,‡ Christopher R. Clough§ and Christopher C. Cummins*

Received 9th January 2015,
Accepted 12th February 2015

DOI: 10.1039/c5dt00105f

www.rsc.org/dalton

This work explores the reduction of 4,4′-bipyridine using two equivalents of the titanium(III) complex $Ti(N[^tBu]Ar)_3$ resulting in formation of a black, crystalline complex, (4,4′-bipy){$Ti(N[^tBu]Ar)_3$}$_2$, for which an X-ray structure determination is reported. The neutral, black, 4,4′-bipyridine-bridged bimetallic was found to be redox active, with mono- and di-anions being accessible electrochemically, and with the mono- and di-cations also being accessible chemically, and isolable, at least when using the weakly coordinating anion $[B(C_6F_5)_4]^-$ as the counter-ion. It proved possible to crystallize the salt [(4,4′-bipy){$Ti(N[^tBu]Ar)_3$}$_2$]-$[B(C_6F_5)_4]_2$ for a single-crystal X-ray structure investigation; in this instance it was revealed that the aromaticity of the 4,4′-bipyridine ligand, that had been disrupted upon reduction, had been regained. A rare cationic d^0 metal tris-amide complex, shown by X-ray crystallography to contain an intriguing pyramidal TiN_3 core geometry, namely $\{Ti(N[^tBu]Ar)_3\}^+$, could also be isolated when using $[B(C_6F_5)_4]$ as the essentially non-interacting counter-ion. This highly reactive cation should be considered as a potential intermediate in the plethora of reactions wherein $Ti(N[^tBu]Ar)_3$ has been shown to effect the reduction of substrates including halogenated organic molecules, carbonyl compounds, organic nitriles, and metal complexes.

1 Introduction

This investigation took shape as an inquiry into the potential ability of the tris-anilide titanium(III) complex $Ti(N[^tBu]Ar)_3$ (Ar = 3,5-$Me_2C_6H_3$) to reductively bind or couple pyridine. Pyridine coupling as a route to bipyridines is a reaction of significant interest, and it has been shown previously by Rothwell *et al.* that pyridine reductive coupling could be effected by a titanium(II) synthon resulting in a dititanium(III) system containing a bridging {–$NC_4H_4C(H)$–$C(H)C_4H_4N$–} moiety.[1] In addition, we showed previously that $Ti(N[^tBu]Ar)_3$ was capable of promoting pyridine reductive cross-coupling with benzonitrile, with the molybdenum(III) tris-anilide complex Mo-$(N[^tBu]Ar)_3$ in this case responsible for reductive complexation of the organic nitrile prior to coupling with titanium-complexed pyridine.[2] Related to Rothwell's *para*-coupled pyridine dimer by dehydrogenation is a system in which 4,4′-bipyridine bridges two titanium centers, and accordingly, this article treats the ability of $Ti(N[^tBu]Ar)_3$ (Fig. 1) to reductively complex that organic molecule in a 2 : 1 fashion. A study of the redox behavior of the (4,4′-bipy){$Ti(N[^tBu]Ar)_3$}$_2$ bimetallic system led to the significant discovery that the highly electrophilic cation {Ti-$(N[^tBu]Ar)_3$}$^+$ could be isolated when generated in particular as its $\{[B(C_6F_5)_4]\}^-$ salt. The synthesis and structural characterization of cation $\{Ti(N[^tBu]Ar)_3\}^+$ is a key finding delivered in the present work, as this species is a plausible reactive intermediate in a variety of reductive processes effected by the special one-electron reducing agent that is embodied by $Ti(N[^tBu]Ar)_3$.

1.1 Reductions effected by titanium tris-anilide

As a one-electron reducing agent, $Ti(N[^tBu]Ar)_3$ may be compared to SmI_2,[4] but in general $Ti(N[^tBu]Ar)_3$ is "hotter" in being able to effect halogen atom abstraction from less-activated halogen-containing organic molecules than SmI_2 is capable of; an example of this is X abstraction from stoichio-

6-435 Department of Chemistry, Massachusetts Institute of Technology, 77 Massachusetts Avenue, Cambridge, MA 02139-4307, USA.
E-mail: ccummins@mit.edu; Tel: +(617) 253-5332

†Electronic supplementary information (ESI) available: Spectra, tables of crystallographic data, DFT-optimized coordinates. CCDC 893531–893535. For ESI and crystallographic data in CIF or other electronic format see DOI: 10.1039/C5DT00105F

‡Present address: The Dow Chemical Company, 1776 Building, Midland, MI 48674, USA.
§Present address: SAFC Hitech, 5485 County Road V, Sheboygan Falls, WI 53085, USA.

This journal is © The Royal Society of Chemistry 2015

Open Access Article. Published on 16 February 2015. Downloaded on 8/23/2022 12:27:23 PM.
This article is licensed under a Creative Commons Attribution 3.0 Unported Licence.

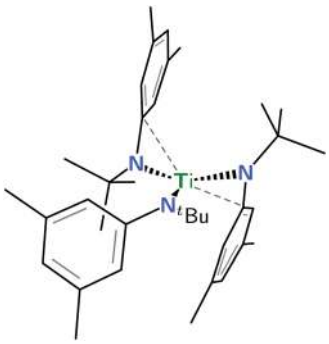

Fig. 1 Line drawing of neutral Ti(N[^{t}Bu]Ar)$_3$ based upon coordinates from an X-ray crystal structure[3] and emphasizing (dashed lines) the two aryl groups that make close contact with the electrophilic d^1 metal center.

metric bromobenzene or iodobenzene to produce the corresponding titanium(IV) complex XTi(N[^{t}Bu]Ar)$_3$ rapidly and quantitatively at 25 °C in a nonpolar solvent such as benzene.[5] While 7-chloronorbornadiene similarly gave a rapid reaction,[6] neat chlorobenzene proved to be less reactive, requiring *ca.* 8 h to produce ClTi(N[^{t}Bu]Ar)$_3$ (also in essentially quantitative yield), while fluorobenzene was observed to be effectively inert to Ti(N[^{t}Bu]Ar)$_3$.[5] Since Ti(N[^{t}Bu]Ar)$_3$ has little propensity to capture organic radicals, its halogen abstraction propensity could be harnessed in a radical synthesis of PR_3 molecules utilizing white phosphorus.[7] In general, carbonyl compounds are attacked rapidly by Ti(N[^{t}Bu]Ar)$_3$ leading to ketyl radical chemistry;[5] this behavior is similar to that reported by Covert and Wolczanski for the related three-coordinate titanium(III) complex Ti(OSi^{t}Bu$_3$)$_3$.[8] *tert*-Butyl esters react giving substitution of *tert*-butyl radical by Ti(N[^{t}Bu]Ar)$_3$, a facile pathway for the synthesis of formate derivatives.[9] Titanium tris-anilide has also been shown to reduce inorganic substrates, for example in the synthesis of $WCl_3(THF)_3$ from $WCl_4(DME)$,[10] in the reductive complexation of metal oxo and nitrido systems,[3,11] and in the synergistic (together with Mo(N[^{t}Bu]Ar)$_3$) binding of N_2.[12] Additionally, there is evidence that Ti(N[^{t}Bu]Ar)$_3$ engages in (reversible) reductive complexation of CO_2 and pyridine.[2]

2 Results and discussion

2.1 Reaction of Ti(N[^{t}Bu]Ar)$_3$ with 4,4′-bipyridine

The dinuclear titanium complex (4,4′-bipy){Ti(N[^{t}Bu]Ar)$_3$}$_2$ was synthesized in excellent yield (89%) *via* treatment of a bright green solution of Ti(N[^{t}Bu]Ar)$_3$ in thawing Et_2O (−110 °C) with 0.5 equiv. of 4,4′-bipyridine. Addition of the latter reactant elicited a color change from green to black and then the product (4,4′-bipy){Ti(N[^{t}Bu]Ar)$_3$}$_2$ precipitated as a fine black powder. The bimetallic complex is diamagnetic, and its structure (a single anilide ligand environment and D_{2h} symmetry of the bridging 4,4′-bipyridine ligand) was readily assigned using ^{1}H and ^{13}C NMR spectroscopies. Integration of ^{1}H NMR signals indicated that there were six anilide ligands for every one molecule of 4,4′-bipyridine. The complex is diamagnetic by virtue of two electron reduction of the 4,4′-bipyridine bridge by the two equivalents of titanium(III) tris-anilide; the ^{1}H NMR chemical shifts observed for the bipyridine protons (δ = 5.43 and 6.97 ppm) are typical of those observed in other doubly reduced 4,4′-bipyridine species.[13,14]

2.2 Molecular structure of (4,4′-bipy){Ti(N[^{t}Bu]Ar)$_3$}$_2$

Crystals of (4,4′-bipy){Ti(N[^{t}Bu]Ar)$_3$}$_2$ that were grown from a saturated toluene solution were found to be suitable for analysis by X-ray crystallography; the space group was $P\bar{1}$ with a crystallographic inversion center located at the midpoint of the central C–C bond. The observed molecular structure of (4,4′-bipy){Ti(N[^{t}Bu]Ar)$_3$}$_2$ confirms the presence of a reduced 4,4′-bipyridine bridge in the molecule (Fig. 2). The central C–C bond is markedly contracted (1.394(2) Å) relative to the single C–C bond in free 4,4′-bipyridine (1.484(2) Å), and is essentially equal in length to the double C–C bond observed in bis(trimethylsilyl)dihydro-4,4′-bipyridine (1.382(3) Å), another doubly-reduced derivative of 4,4′-bipyridine.[13,14] The shortest C–C distance observed in the pyridyl rings of the complex (C41–C42 = 1.358(2) Å) also points to the existence of localized C–C double bonds in the molecule. The Ti1–N4 distance (1.9913(13) Å) is similar to the average Ti1–N distance for the anilide ligands (1.97 Å), indicating that N4 may be regarded similarly as an amide nitrogen atom, as would be expected in a system containing a [4,4′-bipyridine]$^{2-}$ moiety. A search of the Cambridge Structural Database returned one other system containing two titanium atoms bridged by a 4,4′-bipyridine ligand. In 2005, Kraft *et al.* reported a molecular square

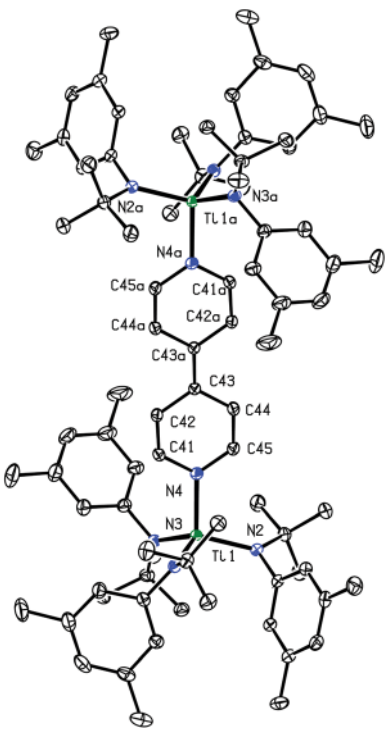

Fig. 2 Diagram of (4,4′-bipy){Ti(N[^{t}Bu]Ar)$_3$}$_2$ with thermal ellipsoids at the 50% probability level.[15]

Open Access Article. Published on 16 February 2015. Downloaded on 8/23/2022 12:27:23 PM.
This article is licensed under a Creative Commons Attribution 3.0 Unported Licence.

formed from four molecules of 4,4′-bipyridine connected by four titanocene fragments at the corners.[14] In this case the 4,4′-bipyridine ligands were only partially reduced, with interatomic distances intermediate between those of neutral 4,4′-bipyridine and bis(trimethylsilyl)dihydro-4,4′-bipyridine.

2.3 Electronic structure of (4,4′-bipy){Ti(N[^{t}Bu]Ar)$_3$}$_2$

To gain insight into the electronic structure of the neutral dititanium complex of 4,4′-bipyridine, density functional theory (DFT) calculations were performed on a truncated version of the molecule: (4,4′-bipy){Ti(N[Me]Ph)$_3$}$_2$; the model was built based upon the crystallographic atomic coordinates for (4,4′-bipy){Ti(N[^{t}Bu]Ar)$_3$}$_2$ and then geometry-optimized. The calculated HOMO (Fig. 3) contains both π-bonding and π-antibonding character, with the most significant contribution coming from the central C–C π-bond; the pattern of π bonding in the HOMO corresponds nicely to what is likely the dominant Lewis resonance structure for this system. Notably, the HOMO also contains a contribution from Ti–N π-bonding. The LUMO is composed almost exclusively of metal-centered empty d orbital character. A significant HOMO–LUMO energy gap is predicted by the calculation (0.83 eV) and this is supported by

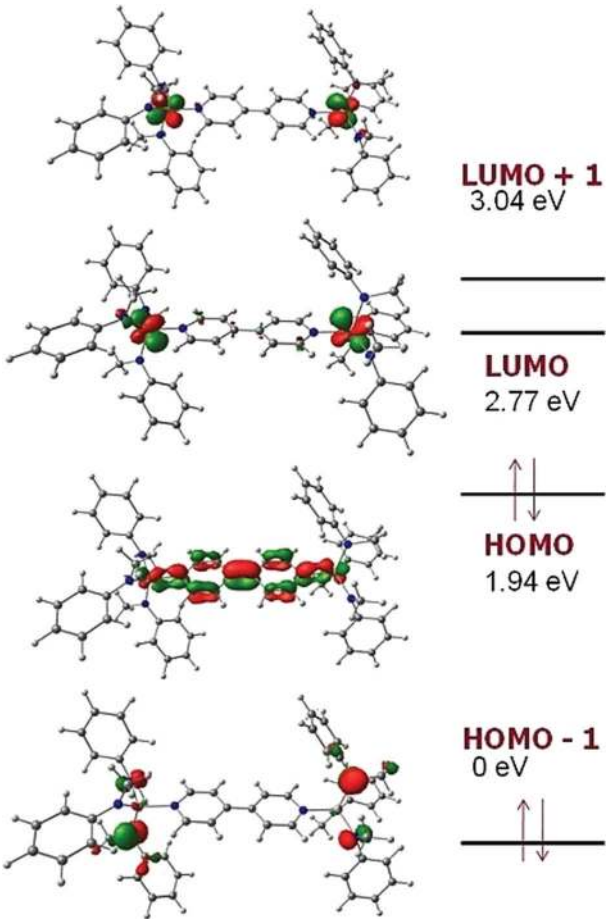

Fig. 3 Frontier MO energy levels calculated for model system (4,4′-bipy){Ti(N[Me]Ph)$_3$}$_2$.[16]

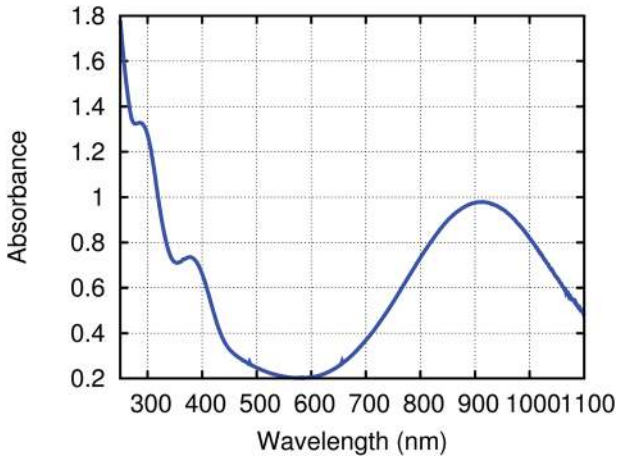

Fig. 4 Electronic absorption spectrum of (4,4′-bipy){Ti(N[^{t}Bu]Ar)$_3$}$_2$ as a solution in THF.

the presence of a strong ligand-to-metal charge transfer band at 910 nm (ε = 32 000 M^{-1} cm^{-1}) in the UV/Vis spectrum of black (4,4′-bipy){Ti(N[^{t}Bu]Ar)$_3$}$_2$ (Fig. 4).

2.4 Electrochemistry and chemical redox of (4,4′-bipy){Ti(N[^{t}Bu]Ar)$_3$}$_2$

The electronic structure of (4,4′-bipy){Ti(N[^{t}Bu]Ar)$_3$}$_2$ leads to interesting electrochemical behavior in solution. Cyclic voltammetry performed on THF solutions of (4,4′-bipy){Ti(N[^{t}Bu]-Ar)$_3$}$_2$ (Fig. 5) indicates two reversible oxidation events and two quasi reversible reduction events and the electrochemical data are summarized in Table 1. The observed redox features can be explained by considering the different charged states of the molecule (illustrated in Fig. 6 for the isolable neutral, cationic, and di-cationic species). Starting from the neutral species, removal of an electron from the [4,4′-bipy]$^{2-}$ ligand results in formation of a radical cation without any change to titanium oxidation state. Nevertheless, it is possible to draw a resonance structure for this species wherein the unpaired electron resides on one of the titanium centers, such that the radical cation could also be formulated as a mixed-valent titanium(III)/titanium(IV) species. Removal of an additional electron from the radical cation leads to dicationic [(4,4′-bipy){Ti(N[^{t}Bu]-Ar)$_3$}$_2$]$^{2+}$, in which aromaticity is restored to the bridging 4,4′-bipy ligand.

Sweeping negative, addition of an electron to (4,4′-bipy){Ti(N[^{t}Bu]Ar)$_3$}$_2$ converts one of the titanium(IV) centers in the molecule to titanium(III) and generates an anionic mixed-valent complex. Addition of a second electron reduces the remaining titanium(IV) center to titanium(III). It is indicated that all five charge states of (4,4′-bipy){Ti(N[^{t}Bu]Ar)$_3$}$_2$ should be accessible through chemical oxidation and reduction reactions, with the exception of the second reduction event. At −2.7 V *vs.* the Fc/Fc$^+$ couple, the latter is too near the solvent window. Here we note that the cyclic voltammogram of bis(trimethylsilyl)dihydro-4,4′-bipyridine exhibits two reversible oxidation waves at potentials (*vs.* Fc/Fc$^+$) nearly identical to those

 This journal is © The Royal Society of Chemistry 2015

Open Access Article. Published on 16 February 2015. Downloaded on 8/23/2022 12:27:23 PM.
This article is licensed under a Creative Commons Attribution 3.0 Unported Licence.

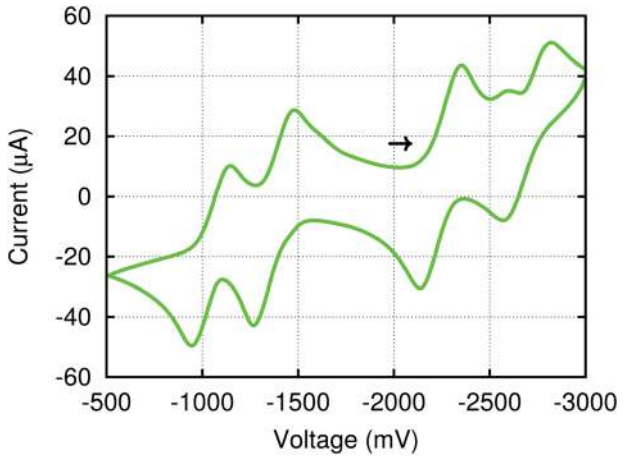

Fig. 5 Cyclic voltammogram for (4,4′-bipy){Ti(N[^{t}Bu]Ar)$_3$}$_2$ in THF with a sweep rate of 800 mV s^{-1} referenced *vs.* Fc/Fc$^+$ with [N^{n}Bu$_4$][B(C$_6$F$_5$)$_4$] (0.2 M) as the supporting electrolyte. The arrow signifies the rest potential and the direction of the sweep.

Table 1 Electrochemical data for the complex (4,4′-bipy){Ti(N[^{t}Bu]-Ar)$_3$}$_2$

Couple	$E_{1/2}$/V[a]	$\Delta E_{1/2}$/V[b]	K_c[c]
2−/1−	−2.65	0.43	1.9×10^7
1−/0	−2.22		
0/1+	−1.36	0.32	2.6×10^5
1+/2+	−1.04		

[a] $E_{1/2}$ values are referenced *versus* ferrocene/ferrocenium. [b] Separation between two adjacent half-wave potentials representing the range wherein the respective ion exists. [c] Calculated according to $\ln K_c = -nF\Delta E_{1/2}/RT$.[17]

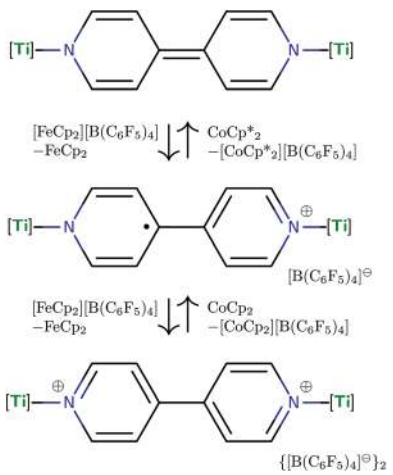

Fig. 6 Isolable in three states of charge, the figure depicts schematically (4,4′-bipy){Ti(N[^{t}Bu]Ar)$_3$}$_2$, its mono-cation, and di-cation, the latter cations both having been isolated as perfluoro-tetraphenyl borate salts.

observed here;[13] however, for that molecule the two reversible reduction waves are absent as there are present at silicon vis-à-vis titanium no low-lying empty d orbitals.

Differential pulse voltammetry (DPV)[18] was used to obtain accurate $E_{1/2}$ values for each of the one-electron couples observed in the cyclic voltammogram. The comproportionation constants K_c were calculated for the proposed mixed-valence species [(4,4′-bipy){Ti(N[^{t}Bu]Ar)$_3$}$_2$]$^+$ in order to evaluate the extent of electronic communication between the titanium centers. The K_c values were derived from the potential separation between $\Delta E_{1/2}$ between couples (Table 1).[17] For the cation [(4,4′-bipy){Ti(N[^{t}Bu]Ar)$_3$}$_2$]$^+$, the $\Delta E_{1/2}$ value of 0.32 V corresponds to $K_c = 2.6 \times 10^5$, which is in the range usually associated with Class II mixed-valent compounds.[19] Therefore, some degree of electronic communication is occurring between the two metal centers. This communication is more pronounced in the anion, [(4,4′-bipy){Ti(N[^{t}Bu]Ar)$_3$}$_2$]$^-$, where the larger $\Delta E_{1/2}$ value of 0.43 V corresponds to $K_c = 1.9 \times 10^7$. A greater degree of electronic delocalization is therefore observed in the mixed-valent anion than in the mixed-valent cation.

Chemical oxidation reactions of (4,4′-bipy){Ti(N[^{t}Bu]Ar)$_3$}$_2$ have shown that it is possible to release an equivalent of 4,4′-bipyridine from the molecule. For example, treatment of (4,4′-bipy){Ti(N[^{t}Bu]Ar)$_3$}$_2$ with an equivalent of iodine resulted in its quantitative conversion to two equivalents of ITi(N[^{t}Bu]-Ar)$_3$ [5,11] with concomitant release of an equivalent of 4,4′-bipyridine. A similar transformation was also achieved with two equivalents of the outer-sphere oxidant ferrocenium triflate (Fc[OTf]), and demonstrates that the reduction of 4,4′-bipyridine by titanium(III) trisanilide Ti(N[^{t}Bu]Ar)$_3$ is chemically reversible. Treatment of (4,4′-bipy){Ti(N[^{t}Bu]Ar)$_3$}$_2$ with a single equivalent of Fc[OTf] did not result in conversion to a one-electron oxidation product, but instead, half an equivalent of the dinuclear complex was consumed in being oxidized by two electrons, leaving half an equivalent unreacted. This is not entirely surprising considering how closely spaced the two oxidation events are in the cyclic voltammogram and that only mild oxidizing agents are required for both transformations.

The one-electron oxidation product [(4,4′-bipy){Ti(N[^{t}Bu]-Ar)$_3$}$_2$]$^+$ is available *via* oxidation with a ferrocenium salt containing a weakly coordinating anion. For example, treatment of (4,4′-bipy){Ti(N[^{t}Bu]Ar)$_3$}$_2$ with one equivalent of Fc[B(C$_6$F$_5$)$_4$] [20,21] at room temperature in THF resulted upon mixing in a color change from black to brown. After separation from ferrocene, the [B(C$_6$F$_5$)$_4$]$^-$ salt of [(4,4′-bipy){Ti(N[^{t}Bu]Ar)$_3$}$_2$]$^+$ was isolated as a brown powder (84% yield). The latter cation proved to be completely NMR silent. It also was found to be sensitive thermally, appearing gradually to decompose in solution at room temperature over a period of a few days. Efforts to grow crystals of this salt at low temperature did not succeed.

The radical nature of [(4,4′-bipy){Ti(N[^{t}Bu]Ar)$_3$}$_2$]$^+$ was confirmed by EPR spectroscopy. A room-temperature EPR spectrum of a toluene solution containing the cation displayed only one signal (g = 2.0004), with no additional hyperfine coupling. The g-value of the signal is typical of an organic π-radical; however, this does not rule out a resonance contributor to the radical cation in which the unpaired electron is located on one of the titanium ions. As the HOMO of the neutral precursor is largely π-bonding in nature, removal of an

Open Access Article. Published on 16 February 2015. Downloaded on 8/23/2022 12:27:23 PM.
This article is licensed under a Creative Commons Attribution 3.0 Unported Licence.

electron from this orbital should result in π bonds of reduced order. Consistent with this, the IR spectrum of [(4,4′-bipy)-{Ti(N[^{t}Bu]Ar)$_3$}$_2$]$^+$ (as its [B(C$_6$F$_5$)$_4$]$^-$ salt) displays a C=C stretch at 1614 cm^{-1}, compared to the C=C stretch at 1622 cm^{-1} that is observed for the neutral precursor. Additionally, the UV/Vis spectrum of the radical cation in THF shows a band at 965 nm (ε = 10 000 M^{-1} cm^{-1}), this being less intense than the corresponding band observed at 910 nm (ε = 32 000 M^{-1} cm^{-1}) in the unoxidized species. This can be interpreted as a diminution of the LMCT interaction in the system upon oxidation.

In line with the inference that one-electron oxidation of (4,4′-bipy){Ti(N[^{t}Bu]Ar)$_3$}$_2$ is not accompanied by any major structural change, we found that the cation [(4,4′-bipy){Ti-(N[^{t}Bu]Ar)$_3$}$_2$]$^+$ can be reduced back to its neutral and diamagnetic precursor by treatment with decamethyl cobaltocene. The cation can also be further oxidized by treatment with an additional equivalent of Fc[B(C$_6$F$_5$)$_4$] to yield the new dicationic complex [(4,4′-bipy){Ti(N[^{t}Bu]Ar)$_3$}$_2$]$^{2+}$ as its ([B(C$_6$F$_5$)$_4$]$^-$)$_2$ salt. The latter red salt, as expected, could also be accessed (in 84% yield) upon treatment of (4,4′-bipy){Ti(N[^{t}Bu]Ar)$_3$}$_2$ with two equivalents of Fc[B(C$_6$F$_5$)$_4$]. Additionally, two equiv. of the radical cation [(4,4′-bipy){Ti(N[^{t}Bu]Ar)$_3$}$_2$]$^+$ are generated quantitatively upon mixing of one equivalent each of neutral (4,4′-bipy){Ti(N[^{t}Bu]Ar)$_3$}$_2$ and [(4,4′-bipy){Ti(N[^{t}Bu]Ar)$_3$}$_2$]$^{2+}$, demonstrating the relationship among this series of complexes whose compositions differ only in terms of their state of charge.

Crystals of the ([B(C$_6$F$_5$)$_4$]$^-$)$_2$ salt of dication [(4,4′-bipy){Ti-(N[^{t}Bu]Ar)$_3$}$_2$]$^{2+}$ suitable for an X-ray diffraction study were grown by liquid–liquid diffusion of hexane into an *o*-difluorobenzene solution. *o*-Difluorobenzene is polar and has a higher dielectric constant (D_s = 13.8) than THF (D_s = 7.4), but is a weaker donor.[22] The ([B(C$_6$F$_5$)$_4$]$^-$)$_2$ salt of dication [(4,4′-bipy)-{Ti(N[^{t}Bu]Ar)$_3$}$_2$]$^{2+}$ is insoluble in alkane and arene solvents, but dissolves in coordinating solvents including THF and pyridine. However, dissolution in pyridine-d$_5$ results in a ligand displacement reaction, liberating 4,4′-bipyridine and resulting in coordination of pyridine-d$_5$ to the liberated {Ti(N[^{t}Bu]Ar)$_3$}$^+$ moieties (*vide infra*). When the dication salt is dissolved in THF-d$_8$, the THF-d$_8$ solvent molecules compete with 4,4′-bipyridine for binding to the {Ti(N[^{t}Bu]Ar)$_3$}$^+$ cations, resulting in an equilibrium between free and bound 4,4′-bipyridine being observed in the solution ^{1}H NMR (benzene-d$_6$, 20 °C, 500 MHz) spectrum. Thus, the use of *o*-difluorobenzene as a crystallization solvent was key to determining the solid-state structure of the dication's ([B(C$_6$F$_5$)$_4$]$^-$)$_2$ salt. The molecular structure of dication [(4,4′-bipy){Ti(N[^{t}Bu]Ar)$_3$}$_2$]$^{2+}$ is shown in Fig. 7.

The most striking structural feature of dication [(4,4′-bipy)-{Ti(N[^{t}Bu]Ar)$_3$}$_2$]$^{2+}$ is the twist about the central C–C bond of the bipyridine (torsion angle = 37.16°). A twist of similar magnitude is observed in free 4,4′-bipyridine (torsion angle = 34.20°).[14] Additionally, the central C–C bond is 1.484(4) Å in length, coincident with the corresponding distance in free 4,4′-bipyridine (1.484(2) Å) and 0.09 Å longer than in neutral (4,4′-bipy){Ti(N[^{t}Bu]Ar)$_3$}$_2$ (1.394(2) A). This demonstrates that the removal of two electrons from (4,4′-bipy){Ti(N[^{t}Bu]Ar)$_3$}$_2$ results

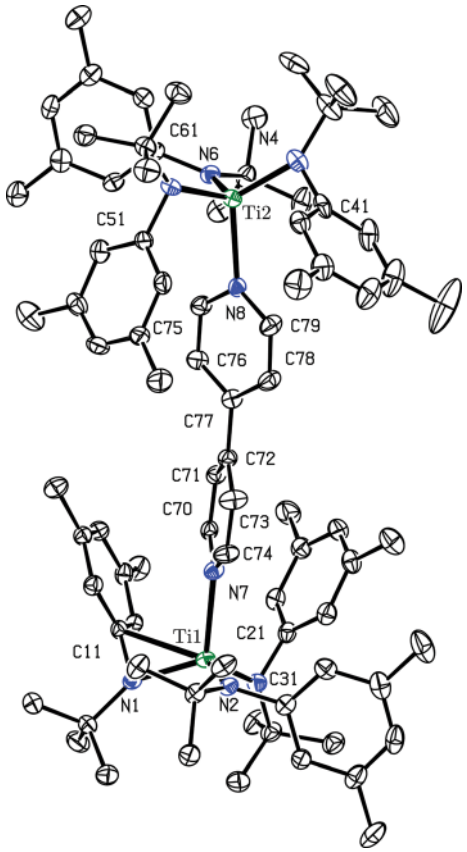

Fig. 7 Diagram (50% probability ellipsoids) of dication [(4,4′-bipy){Ti-(N[^{t}Bu]Ar)$_3$}$_2$]$^{2+}$ with hydrogen atoms, [B(C$_6$F$_5$)$_4$]$^-$ ions, and an *o*-difluorobenzene solvent molecule omitted.[15]

in rearomatization of the 4,4′-bipyridine unit. In further support of the latter interpretation, the Ti–N(bipyridine) distances in [(4,4′-bipy){Ti(N[^{t}Bu]Ar)$_3$}$_2$]$^{2+}$ (2.209(2) Å and 2.213(2) Å) are substantially longer than they are in neutral (4,4′-bipy)-{Ti(N[^{t}Bu]Ar)$_3$}$_2$ (1.9913(13) Å), and are characteristic of the interaction between a neutral N-donor and titanium(IV).[23] Compensating for the weaker Ti–N(bipyridine) bonds, the Ti–N(anilide) distances in the dication (avg. = 1.92 Å) are substantially shorter than in the neutral precursor (avg. = 1.97 Å), consistent with increased π-donation to the cationic titanium centers from the anilide nitrogens. As well, there appears to be an additional bonding interaction between C11 and Ti1 (C11···Ti1 = 2.500(3) Å), and C41 also closely approaches Ti2 (C41···Ti2 = 2.554(3) Å). It is not unprecedented for *N-tert*-butylanilide ligands to bind in an η^2 or even in an η^3 fashion in the process of stabilizing an electrophilic metal center.[3]

2.5 Synthesis and molecular structure of cation {Ti(N[^{t}Bu]-Ar)$_3$}$^+$ ([B(C$_6$F$_5$)$_4$]$^-$ salt)

The dication of the previous section can reasonably be viewed as two {Ti(N[^{t}Bu]Ar)$_3$}$^+$ cations linked by a neutral 4,4′-bipyridine ligand. As the {Ti(N[^{t}Bu]Ar)$_3$}$^+$ cation had never been independently synthesized in our laboratory, we set out to accomplish this *via* oxidation of Ti(N[^{t}Bu]Ar)$_3$ using [FeCp$_2$]-

 This journal is © The Royal Society of Chemistry 2015

Open Access Article. Published on 16 February 2015. Downloaded on 8/23/2022 12:27:23 PM.
This article is licensed under a Creative Commons Attribution 3.0 Unported Licence.

$[B(C_6F_5)_4]$. Treatment of a green, ethereal solution of $Ti(N[^tBu]Ar)_3$ with an Et_2O slurry of $[FeCp_2][B(C_6F_5)_4]$ at room temperature resulted upon mixing in a color change to red. After removal of solvent under reduced pressure, what remained was a red oil that could be converted to an orange powder upon repeated trituration using *n*-hexane. The orange powder was determined to be the salt $\{Ti(N[^tBu]Ar)_3\}[B(C_6F_5)_4]$, obtained (90% yield) in a form that is entirely free of any coordinating solvent molecules. In this form, salt $\{Ti(N[^tBu]Ar)_3\}[B(C_6F_5)_4]$ is insoluble in Et_2O, benzene and toluene, but does dissolve in these solvents upon addition of a few drops of THF. The relative inertness of the $[B(C_6F_5)_4]^-$ counter-ion is key to the isolation of the $\{Ti(N[^tBu]Ar)_3\}^+$ cation. Prior experiments aimed at similarly generating the cation $\{Ti(N[^tBu]Ar)_3\}^+$ *via* ferrocenium oxidation using $[FeCp_2][B[3,5\text{-}C_6H_3(CF_3)_2]_4]$[24] instead resulted in isolation of the fluoride, $FTi(N[^tBu]Ar)_3$.[5] It is likely that the reactive $\{Ti(N[^tBu]Ar)_3\}^+$ cation is formed under the latter conditions but that it abstracts fluoride from the insufficiently inert $[B[3,5\text{-}C_6H_3(CF_3)_2]_4]^-$ anion.

Crystals of $\{Ti(N[^tBu]Ar)_3\}[B(C_6F_5)_4]$ were grown by liquid–liquid diffusion of hexane into an *o*-difluorobenzene solution of the salt, conducive to an X-ray diffraction study (Fig. 8). The titanium(IV) ion of cation $[Ti(N[^tBu]Ar)_3]^+$ pulls the *N-tert*-butylanilide ligands in very close (Ti1–N = 1.8788(15), 1.8830(16), and 1.8937(16) Å). Additionally, all three anilide ligands in this otherwise unsolvated cation appear to engage titanium in an η^2-*N*,*C* fashion, with the Ti1–C distances (2.3870(18), 2.3984(18), and 2.4048(19) Å) being shorter than is typically observed for η^2 or η^3 anilide aryl ring ligation to titanium; for example, see the structure of $\{(THF)Ti(N[^tBu]Ar)_3\}^+$, described below (Fig. 9).

A most unusual feature of the structure (Fig. 8) is the trigonal pyramidal nature of the TiN_3 core unit (the average N–Ti–N angle is *ca.* 111.3°); despite the presence of two η^3 anilide interactions in the structure of neutral $Ti(N[^tBu]Ar)_3$,[3] the TiN_3 moiety in that case is rigorously trigonal planar, a structural

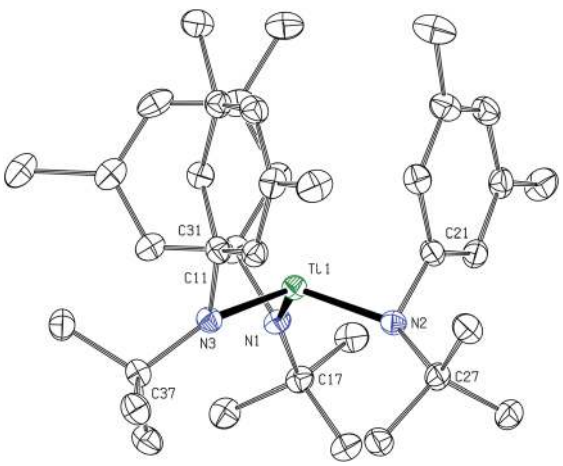

Fig. 8 Diagram of cation $\{Ti(N[^tBu]Ar)_3\}^+$ with 50% probability ellipsoids.[15] The $[B(C_6F_5)_4]^-$ counter-anion and hydrogen atoms are omitted for clarity (no close anion/cation contacts were observed).

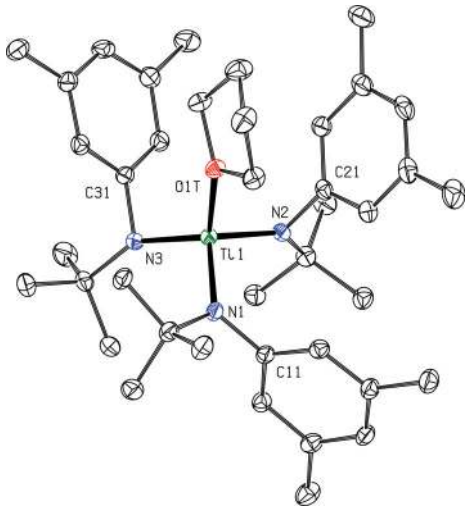

Fig. 9 Diagram of cation $\{(THF)Ti(N[^tBu]Ar)_3\}^+$ with 50% probability ellipsoids.[15] The $[B(C_6F_5)_4]^-$ counter-anion, ether molecule of crystallization and hydrogen atoms are omitted for clarity (no close anion/cation contacts were observed).

feature common to all of the neutral $M(N[R]Ar)_3$ complexes that have been characterized to date (M = Ti,[3] V,[25] Cr,[26] Mo[12,27–29]). Trigonal pyramidal MN_3 units are, however, a characteristic structural feature for homoleptic rare earth metal phenyl(trimethylsilyl) amide complexes.[30] In addition, Andersen has remarked on the trigonal pyramidal coordination environment at uranium in $U[N(SiMe_3)_2]_3$.[31] Finally, Hursthouse *et al.* showed that the coordination environment at scandium in $Sc[N(SiMe_3)_2]_3$ is similarly trigonal pyramidal with N–Sc–N angles of *ca.* 117°.[32]

The *N-tert*-butylanilide ligands in the otherwise unsolvated $[Ti(N[^tBu]Ar)_3]^+$ cation can certainly be viewed as providing a protective steric sheath about the electrophilic titanium(IV) center that is essential, together with the inert counter anion, for its isolation. Inspection of the packing arrangement in this crystal structure reveals no significant cation–anion interactions.

2.6 Electronic structure of cation $\{Ti(N[^tBu]Ar)_3\}^+$

The trigonal pyramidal nature of $\{Ti(N[^tBu]Ar)_3\}^+$ is not the only unusual feature of the observed structure. The Ti–N–CMe_3 angles are quite obtuse (average value, 147.08°) while the Ti–N–C(aryl) angles are correspondingly acute (avg.: 91.23°). The latter acute Ti–N–C(aryl) angles bring the three aryl *ipso* carbon atoms in suggestively close to the titanium center, such that structure drawing programs (based on their default element radii) draw lines between Ti1 and each of C11, C21, and C31. The average Ti–C(aryl *ipso*) distance is 2.3967 Å. Because of these relatively close Ti–C(aryl *ipso*) contacts, it is tempting to conclude that there is an associated chemical bonding interaction. In order to probe for this, an Atoms in Molecules (AIM) analysis[33] was carried out on a wavefunction[34] that was calculated at the observed structure (only the hydrogen positions were optimized) with the result that no bond

Open Access Article. Published on 16 February 2015. Downloaded on 8/23/2022 12:27:23 PM.
This article is licensed under a Creative Commons Attribution 3.0 Unported Licence.

critical points were located between titanium and the aryl *ipso* carbon atoms; by this electron density criterion, no chemical bonds exist between titanium and the aryl *ipso* carbon atoms and we must conclude that the relatively close contacts occur incidentally as a consequence of the titanium–nitrogen multiple bonding together with unusual hybridization at nitrogen.

Regarding the Ti–N bonding being multiple in $\{Ti(N[^tBu]Ar)_3\}^+$, natural bond orbital (NBO)[35,36] and natural resonance theory (NRT)[37–39] analysis of the same wavefunction[34] used for AIM leads to the conclusion that each nitrogen is tetravalent (engages in four electron-pair bonds), that the titanium–nitrogen natural bond order is *ca.* 1.96, and that the natural valence at titanium is six (titanium engages in six electron-pair bonds).[40] This analysis also gives Ti–C(aryl *ipso*) bond orders of near zero, consistent with the lack of associated bond critical points from the AIM analysis. The indicated Ti=N double bonding is associated with short titanium–nitrogen interatomic distances (avg.: 1.885 Å; for reference, an average value of 1.928 Å was reported for the corresponding chloride derivative, $ClTi(N[^tBu]Ar)_3$).[41]

2.7 Known metal tris-amide cations

The metal tris-amide cations $[M\{N(SiMe_3)_2\}_3]^+$, where M is zirconium or hafnium, have been generated by methide abstraction using $B(C_6F_5)_3$.[42] The latter cations were studied by X-ray crystallography and found to exhibit short M ← (Si–C) contacts interpreted as weak bonding interactions that serve to stabilize the positive charge in these systems.[42] In view of the AIM and NBO results discussed above for the bonding in similarly trigonal pyramidal $\{Ti(N[^tBu]Ar)_3\}$, the invocation of M ← (Si–C) contacts as the reason for the pyramidal nature of the MN_3 (M = Zr, Hf) unit in these cationic amides may warrant reconsideration. Donor-free, cationic transition-metal tris-amide complexes are otherwise unknown. An example of a donor-stabilized titanium tris-amide cation that has been characterized crystallographically is the simple homoleptic dimethylamide-derived system $[(Me_2NH)Ti(NMe_2)_3]^+$ of importance in alkyne carboamination catalysis.[43] A cationic titanium ferrocene-diamide system has been generated by reaction of a dimethyl precursor with the trityl borate $[CPh_3][B(C_6F_5)_4]$ reagent.[44]

2.8 Binding and ring-opening of tetrahydrofuran

We hypothesized that the highly electrophilic titanium(IV) center in the $\{Ti(N[^tBu]Ar)_3\}^+$ cation might allow us to access some previously inaccessible species, one target of interest being the neutral titanium(IV) hydride, $HTi(N[^tBu]Ar)_3$. If obtained, the latter would be a member of the small set of documented titanium(IV) hydride complexes that includes $HTi(ODipp)_3(PMe_3)$,[45] where Dipp represents 2,6-C_6H_3-$^iPr_2$, as well as $\{HTiCp^*(NP^tBu_3)(THF)\}^+$.[46] Addition of stoichiometric [Li][$HBEt_3$] (as a 1.0 M solution in THF) to a thawing red solution of $\{Ti(N[^tBu]Ar)_3\}[B(C_6F_5)_4]$ in *o*-difluorobenzene did not result in any immediate sign of reaction, but the color of the reaction mixture gradually turned from red to orange to yellow as the solution warmed to room temperature. After workup, a major product could be obtained in 58% yield as a free-flowing yellow powder, characterization of which revealed it to be the *n*-butoxy complex $^nBuOTi(N[^tBu]Ar)_3$ that ostensibly arose by way of hydride attack on a coordinated THF ligand. Complexation by strongly Lewis-acidic metal cations is known to activate THF to nucleophilic attack;[47] In one example, addition of KCp* to the cation $[Cp^*_2Sm(THF)_2]^+$ (as its tetraphenylborate salt) led to THF ring-opening and C–C bond formation, rather than to the formation of the desired product, $SmCp^*_3$.[48]

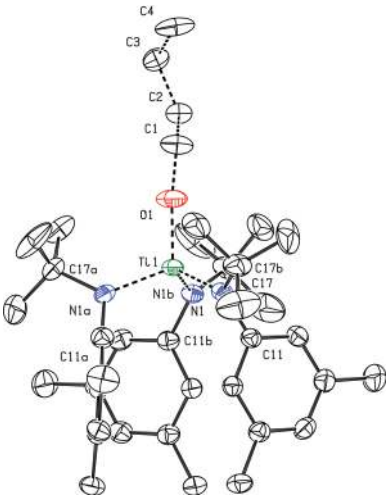

Fig. 10 Diagram of *n*-butoxy complex $^nBuOTi(N[^tBu]Ar)_3$ with 50% probability ellipsoids.[15] The molecule has a crystallographic C_3 axis coincident with the Ti–O vector and the *n*-butyl group occupies two positions (one shown).

2.9 Structure of cation $\{(THF)Ti(N[^tBu]Ar)_3\}^+$

Both the *n*-butoxy complex and the THF adduct $\{(THF)Ti(N[^tBu]Ar)_3\}^+$ (the latter as its $[B(C_6F_5)_4]^+$ salt) have been isolated and characterized by single-crystal X-ray diffraction studies (Fig. 9 and 10). In the case of the cationic THF adduct $\{(THF)Ti(N[^tBu]Ar)_3\}^+$, we find that binding of the THF molecule displaces two of the three Ti···$C_{aryl\,ipso}$ close contacts involving the anilide ligands with respect to the structure observed in the solid state for the solvent-free cation, $\{Ti(N[^tBu]Ar)_3\}^+$ (Fig. 8). The relevant distance that characterizes the remaining Ti1···C31 close contact, 2.5250(16) Å, is longer by greater than 0.1 Å than any of the three such distances observed for $\{Ti(N[^tBu]Ar)_3\}^+$ (Fig. 8). The Ti1–O1 T distance of 2.0962(12) Å characterizing the titanium–THF interaction is not remarkable, but it should be noted that the crystallographic data reported here (Fig. 9) represent rare structural characterization of a group 4 metal cation having the general composition $\{(THF)M(NR^1R^2)_3\}^+$.

3 Experimental details

3.1 General procedures

All manipulations were performed under an atmosphere of purified N_2 in a vacuum atmospheres model MO-40M glovebox or in standard Schlenk glassware in the hood. Solvents were

 This journal is © The Royal Society of Chemistry 2015

Open Access Article. Published on 16 February 2015. Downloaded on 8/23/2022 12:27:23 PM.
This article is licensed under a Creative Commons Attribution 3.0 Unported Licence.

obtained anhydrous and oxygen-free from a Contour Glass Solvent Purification System, built by SG Water recently rebranded as Pure Process Technology (http://www.pureprocesstechnology.com/) with the exception of pyridine which was distilled from sodium. All anhydrous solvents were stored at room temperature over 4 Å molecular sieves. Deuterated solvents were purchased from Cambridge Isotope Labs. Benzene-d_6 was degassed and stored over molecular sieves for at least two days prior to use. THF-d_8 was distilled from sodium/benzophenone and stored over molecular sieves at −35 °C. Pyridine-d_5 was distilled from calcium hydride and stored over molecular sieves. Celite 435 (EM Science), 4 Å molecular sieves (Aldrich), and alumina (EM Science) were dried by heating at 200 °C under a dynamic vacuum for at least 24 hours prior to use. All glassware was oven-dried at temperatures greater than 170 °C prior to use. Ti(N[^{t}Bu]Ar)$_3$ was synthesized following a reported literature procedure[11] that has also been the subject of a video (see http://web.mit.edu/ccclab/videos/). Ferrocenium triflate was prepared by oxidation of ferrocene with silver triflate in dichloromethane.[49] All other chemicals were purchased from Aldrich and used without further purification unless otherwise stated. NMR spectra were obtained on Bruker Avance 400, Varian Mercury 300 or Varian Inova 500 spectrometers. ^{1}H NMR spectra were referenced internally to residual solvent resonances (benzene-d_6, 7.16 ppm; THF-d_8, 3.58 ppm; pyridine-d_5, 8.74 ppm). ^{13}C NMR spectra were referenced internally to solvent signals (benzene-d_6, 128.39 ppm; THF-d_8, 67.57 ppm). ^{19}F NMR spectra were referenced externally to $CFCl_3$. EPR spectra were collected on a Bruker EMX spectrometer outfitted with 13-inch magnets, an ER 4102ST cavity and a Gunn diode microwave source producing X-band (8–10 GHz) radiation. Samples for IR spectroscopy were prepared as Nujol mulls on KBr windows and IR spectra were collected on a Perkin-Elmer 2000 FT-IR spectrophotometer. UV/Vis spectra were collected on a HP8453 spectrophotometer using 1 cm quartz cells manufactured by Starna. Elemental analyses were performed by Midwest Microlab, LLC, Indianapolis, Indiana.

3.2 Preparation of (4,4′-bipy){Ti(N[^{t}Bu]Ar)$_3$}$_2$

Ti(N[^{t}Bu]Ar)$_3$ (3.01 g, 5.22 mmol) was dissolved in 60 mL of Et_2O to create an emerald green solution. This solution was frozen in the dry box cold well. The 4,4′-bipyridine (0.405 g, 2.59 mmol) was dissolved in 15 mL of Et_2O to create a colorless solution. This solution was also frozen in the dry box cold well. The thawing bipyridine slurry (4,4′-bipyridine is insoluble in Et_2O at low temperatures) was added dropwise with stirring to the thawing Ti(N[^{t}Bu]Ar)$_3$ solution. There was an immediate color change from green to black upon addition. The reaction mixture was allowed to stir for one hour while it slowly warmed to room temperature. The Et_2O was removed under vacuum, and the resulting black residue was slurried in 50 mL of *n*-hexane. The black solid was isolated by filtration and washed with *n*-hexane until the washings became colorless. The powder was further dried under dynamic vacuum for two hours. Total yield: 3.12 g, 2.38 mmol, 89% (based on $C_{82}H_{116}N_8Ti_2$, 1309.58 g mol^{-1}). Crystals suitable for X-ray diffraction were grown from a saturated solution of the material in toluene, which was left in the freezer at −35 °C for one week. Anal. Calcd: C 75.21; H 8.93; N 8.56. Found: C 74.98; H 8.78; N 8.67. ^{1}H NMR (benzene-d_6, 20 °C, 400 MHz): δ = 7.12 (broad s, 4H, C═C(*H*)–N), 6.97 (s, 12H, *H*Ar), 6.77 (s, 6H, *H*Ar), 5.43 (d, J_{HH} = 8 Hz, 4H, (*H*)C═C–N), 2.34 (s, 36H, Ar–CH_3), 1.23 (s, 54H, C(CH_3)$_3$) ppm. ^{13}C NMR (benzene-d_6, 20 °C, 100.6 MHz): δ = 150.4 (s, aryl *ipso*), 137.3 (s, *m*-Ar), 137.0 (s, central C═C), 129.6 (s, *p*-Ar), 127.3 (s, *o*-Ar), 118.4 (s, ring C═C), 105.7 (s, ring C═C), 63.8 (s, NC(*C*H$_3$)$_3$), 31.0 (s, Ar*C*H$_3$), 22.1 (s, NC(*C*H$_3$)$_3$) ppm. UV/Vis Data (THF, 3.05 × 10^{-5} M, 20 °C): λ_{max} = 287 nm (ε = 32 000 M^{-1} cm^{-1}), λ_{max} = 379 nm (ε = 19 000 M^{-1} cm^{-1}), λ_{max} = 910 nm (ε = 32 000 M^{-1} cm^{-1}). IR Data (nujol mull, KBr plates): 1623 (s), 1586 (vs), 1354 (s), 1287 (vs), 1182 (vs), 1148 (vs), 1043 (vs), 982 (vs), 937 (vs), 885 (vs), 717 (vs), 686 (s), 638 (vs), 581 (s), 418 (s) cm^{-1}.

3.3 Iodine oxidation of (4,4′-bipy){Ti(N[^{t}Bu]Ar)$_3$}$_2$

Complex (4,4′-bipy){Ti(N[^{t}Bu]Ar)$_3$}$_2$ was dissolved in THF (5 mL) to create a black solution (0.100g, 0.0764 mmol). Iodine (0.020 g, 0.079 mmol) was dissolved in THF (2 mL) to create a red-brown solution. The I_2 solution was added to the titanium solution dropwise with stirring. After 30 seconds of stirring, the reaction mixture turned from black to orange. The reaction mixture was allowed to stir for half an hour at which point the solvent was removed under vacuum. The resulting crude material (orange powder) was dissolved in benzene-d_6 for analysis by ^{1}H NMR spectroscopy. This demonstrated that titanium(IV) iodide complex ITi(N[^{t}Bu]Ar)$_3$ [5] was cleanly formed in quantitative yield, together with free 4,4′-bipyridine. ^{1}H NMR (benzene-d_6, 20 °C, 400 MHz): δ = 8.57 (dd, J_{HH} = 4 Hz and 2 Hz, 4H, C═C(*H*)–N, 4,4′-bipyridine), 6.92 (broad s, 12H, *H*Ar), 6.83 (dd, J_{HH} = 8 Hz, 4H, (*H*)C═C–N, 4,4′-bipyridine), 6.81 (broad s, 6H, *H*Ar), 2.25 (s, 36H, Ar–CH_3), 1.38 (s, 54H, C(CH_3)$_3$) ppm.

3.4 Fc[OTf] reaction with (4,4′-bipy){Ti(N[^{t}Bu]Ar)$_3$}$_2$

Complex (4,4′-bipy){Ti(N[^{t}Bu]Ar)$_3$}$_2$ (0.100 g, 0.0764 mmol) was dissolved in THF (5 mL) to create a black solution. Ferrocenium triflate (Fc[OTf],[49] 0.026 g, 0.078 mmol) was slurried in THF (3 mL) to create a dark blue suspension. The Fc[OTf] suspension was added to the titanium solution dropwise, with stirring. After 30 seconds of stirring, the reaction mixture turned from black to dark red-black. The reaction mixture was allowed to stir for half an hour at which time the solvent was removed under reduced pressure. The resulting crude material (dark red powder) was dissolved in benzene-d_6 for analysis by ^{1}H NMR spectroscopy. It is clear from this analysis that no one-electron oxidation product was formed. Half of the starting material (4,4′-bipy){Ti(N[^{t}Bu]Ar)$_3$}$_2$ was oxidized to produce one equivalent of the triflate complex TfOTi(N[^{t}Bu]Ar)$_3$,[11] one equivalent of ferrocene, and half an equivalent of 4,4′-bipyridine. ^{1}H NMR (benzene-d_6, 20 °C, 400 MHz): δ = 8.57 (dd, J_{HH} = 4 Hz and 2 Hz, 2H, C═C(*H*)–N, 4,4′-bipyridine), 7.12 (broad s, 4H, C═C(*H*)–N, (4,4′-bipy){Ti(N[^{t}Bu]Ar)$_3$}$_2$), 6.97 (s, 6H, *H*Ar, (4,4′-bipy){Ti(N[^{t}Bu]Ar)$_3$}$_2$), 6.83 (dd, J_{HH} = 8 Hz, 2H, (*H*)C═C–

Open Access Article. Published on 16 February 2015. Downloaded on 8/23/2022 12:27:23 PM.
This article is licensed under a Creative Commons Attribution 3.0 Unported Licence.

N, 4,4′-bipyridine), 6.77 (s, 3H, *H*Ar, (4,4′-bipy){Ti(N[^{t}Bu]Ar)$_3$}$_2$), 6.74 (s, 3H, *H*Ar, TfOTi(N[^{t}Bu]Ar)$_3$), 6.56 (broad s, 6H, *H*Ar, TfOTi(N[^{t}Bu]Ar)$_3$), 5.43 (d, J_{HH} = 8 Hz, 2H, (*H*)C=C–N, (4,4′-bipy){Ti(N[^{t}Bu]Ar)$_3$}$_2$), 4.00 (s, 10H, ferrocene), 2.34 (s, 18H, Ar–C*H*$_3$, (4,4′-bipy){Ti(N[^{t}Bu]Ar)$_3$}$_2$), 2.23 s, 18H, Ar–C*H*$_3$, TfOTi (N[^{t}Bu]Ar)$_3$), 1.24 (s, 27H, C(C*H*$_3$)$_3$, TfOTi(N[^{t}Bu]Ar)$_3$), 1.23 (s, 27H, C(C*H*$_3$)$_3$, (4,4′-bipy){Ti(N[^{t}Bu]Ar)$_3$}$_2$) ppm.

3.5 Preparation of [FeCp$_2$][B(C$_6$F$_5$)$_4$]

This salt was prepared using Geiger's reported procedure for Fc[PF$_6$],[21] using [Li(OEt$_2$)$_3$][B(C$_6$F$_5$)$_4$][50] in place of Na[PF$_6$]. In a 100 mL round bottom flask, ferrocene (1.00 g, 5.38 mmol) was suspended in a mixture of water (20 mL) and acetone (8 mL). To this suspension, FeCl$_3$ (1.13 g, 6.95 mmol) was added as a solid, immediately creating a dark green solution and evolving heat. The solution gradually changed from dark green to dark blue as it was stirred for 20 minutes. At this point, the dark blue solution was filtered through Celite and a small amount of additional acetone was used to wash the filter cake. The [Li(OEt$_2$)$_3$][B(C$_6$F$_5$)$_4$] (5.02 g, 5.52 mmol) was added with stirring to the dark blue solution. There was no color change, but a dark blue oil began to form on the sides of the flask. After stirring for 15 minutes, ethanol (10 mL) was added to the reaction mixture, causing precipitation of a dark blue solid. The solid was collected by filtration and washed with water (20 mL) and hexane (20 mL). A second crop of solid was obtained by concentrating the volume of the filtrate to about 15–20 mL on a rotary evaporator and then adding additional ethanol (10 mL). The blue solid thus obtained was collected and washed in a similar manner. The two crops of solid were combined and dried under vacuum for 48 hours. Yield: 3.28 g, 3.79 mmol, 70%. ^{19}F{^{1}H} NMR (THF, 20 °C, 282 MHz): 133 (s), 162 (t, J_{FF} = 21 Hz), 166 (t, J_{FF} = 18 Hz) ppm. Note: the ^{19}F NMR signals show some broadening due to the presence of the paramagnetic Fc$^+$ cation in solution.

3.6 Preparation of [(4,4′-bipy){Ti(N[^{t}Bu]Ar)$_3$}$_2$][B(C$_6$F$_5$)$_4$]

(4,4′-bipy){Ti(N[^{t}Bu]Ar)$_3$}$_2$ (0.500 g, 0.382 mmol) was dissolved in THF (20 mL) to create a black solution. The ferrocenium salt, Fc[B(C$_6$F$_5$)$_4$] (0.330 g, 0.381 mmol), was dissolved in THF (5 mL) to create a dark blue solution. The ferrocenium solution was added dropwise with stirring to the solution of (4,4′-bipy){Ti(N[^{t}Bu]Ar)$_3$}$_2$, the color of which gradually changed from black to brown during the course of the addition. The reaction mixture was allowed to stir for half an hour, at which time all volatile materials were removed under vacuum. The brown oil so obtained was dissolved in Et$_2$O (5 mL) and to the solution was added *n*-hexane (20 mL). All volatile materials were again removed under vacuum, yielding a brown, oily solid. The oily solid was slurried in *n*-hexane (20 mL) and then, again, all volatile materials were removed under reduced pressure, leaving a brown powder. The brown powder was in turn slurried in *n*-hexane (20 mL), and then isolated by filtration. The solids were washed with *n*-hexane until the washings became colorless. (Note: the orange filtrate was concentrated to dryness under vacuum and found to contain ferrocene.) After removal of all volatile materials under reduced pressure, salt [(4,4′-bipy){Ti(N[^{t}Bu]Ar)$_3$}$_2$][B(C$_6$F$_5$)$_4$] was isolated as a brown powder. Yield: 0.6382 g, mmol, 84% (based on C$_{106}$H$_{116}$BN$_8$F$_{20}$Ti$_2$, 1988.62 g mol^{-1}). Anal. Calcd: C 64.02; H 5.88; N 5.63. Found (Try 1): C 59.76; H 5.67; N 4.85. Found (Try 2): C 59.18; H 5.24; N 5.45. Poor analytical results for [(4,4′-bipy){Ti(N[^{t}Bu]Ar)$_3$}$_2$][B(C$_6$F$_5$)$_4$] are likely a result of partial decomposition of the radical cation at room temperature. Attempts to further purify the compound failed. The complex gradually decomposes in solution, even at −35 °C. This is noted by a change in color from brown to green or violet. The salt dissolves in benzene-d$_6$ to form a dark brown solution, but was found to be NMR silent by both ^{1}H and ^{19}F NMR spectroscopy. EPR (toluene, 20 °C): singlet at g = 2.0004. UV/Vis Data (THF, 2.85 × 10^{-5} M, 20 °C): λ_{max} = 372 nm (ε = 20 000 M^{-1} cm^{-1}), λ_{max} = 965 nm (ε = 10 000 M^{-1} cm^{-1}). IR Data (nujol mull, KBr plates): 1614 (vs), 1587 (s), 1356 (vs), 1279 (vs), 1209 (m), 1167 (vs), 1128 (vs), 1045 (s), 1022 (s), 974 (vs), 935 (s), 884 (s), 838 (m), 789 (m), 713 (s), 682 (s), 667 (s), 638 (s), 566 (w), 423 (w) cm^{-1}.

3.7 Preparation of [(4,4′-bipy){Ti(N[^{t}Bu]Ar)$_3$}$_2$][B(C$_6$F$_5$)$_4$]$_2$

(4,4′-bipy){Ti(N[^{t}Bu]Ar)$_3$}$_2$ (0.200 g, 0.153 mmol) was dissolved in THF (10 mL) to create a black solution. The ferrocenium salt, Fc[B(C$_6$F$_5$)$_4$] (0.264 g, 0.305 mmol), was dissolved in THF (5 mL) to create a dark blue solution. The ferrocenium solution was added dropwise with stirring to the (4,4′-bipy){Ti(N[^{t}Bu]Ar)$_3$}$_2$ solution, the color of which gradually changed from black to light red during the course of the addition. The reaction mixture was allowed to stir for half an hour at which time all volatile materials were removed under vacuum. The red oil so obtained was dissolved in Et$_2$O (5 mL) and to the solution was added *n*-hexane (20 mL). Solvent was removed from this mixture under vacuum, yielding a red, oily solid. The oily solid was slurried in *n*-hexane (20 mL) and then the mixture was subjected again to solvent removal under reduced pressure, leaving behind a light red-orange powder. The powder was in turn slurried in *n*-hexane (20 mL), and then isolated by filtration. The solids were washed with *n*-hexane until the washings became colorless. (Note: upon solvent removal under reduced pressure, the orange filtrate was found to contain ferrocene.) After complete solvent removal under reduced pressure, salt [(4,4′-bipy){Ti(N[^{t}Bu]Ar)$_3$}$_2$]-[B(C$_6$F$_5$)$_4$]$_2$ was isolated as a red powder. Yield: 0.341 g, 0.128 mmol, 84% (based on C$_{130}$H$_{116}$B$_2$N$_8$F$_{40}$Ti$_2$, 2667.66 g mol^{-1}). Crystals suitable for X-ray diffraction were grown by dissolving 0.15 g in 1.5 mL of *o*-difluorobenzene. The red solution was transferred to an NMR tube, and *n*-hexane was layered on top. The tube was left undisturbed at room temperature for two weeks, during which time large, red, shard-like crystals grew on the sides of the tube (crystals began to appear after one day). Anal. Calcd: C 58.50; H 4.38; N 4.20. Found: C 58.38; H 4.34; N 4.19. ^{1}H NMR (pyridine-d$_5$, 20 °C, 400 MHz): δ = 8.86 (d, J_{HH} = 6 Hz, 2H, free 4,4′-bipy), 7.81 (d, J_{HH} = 6 Hz, 2H, free 4,4′-bipy), 6.99 (s, 3H, *H*Ar, [(pyridine-d$_5$)Ti(N[^{t}Bu]Ar)$_3$]$^+$), 6.91 (s, 6H, *H*Ar, [(pyridine-d$_5$)Ti(N[^{t}Bu]Ar)$_3$]$^+$), 2.31 (s, 18H, Ar-C*H*$_3$, [(pyridine-

 This journal is © The Royal Society of Chemistry 2015

Open Access Article. Published on 16 February 2015. Downloaded on 8/23/2022 12:27:23 PM.
This article is licensed under a Creative Commons Attribution 3.0 Unported Licence.

d_5)Ti(N[^{t}Bu]Ar)$_3$]$^+$), 1.29 (s, 27H, C(CH_3)$_3$, [(pyridine-d_5)Ti-(N[^{t}Bu]Ar)$_3$]$^+$) ppm.

3.8 [(4,4′-bipy){Ti(N[^{t}Bu]Ar)$_3$}$_2$][B(C$_6$F$_5$)$_4$]: alternative preparation

[(4,4′-bipy){Ti(N[^{t}Bu]Ar)$_3$}$_2$][B(C$_6$F$_5$)$_4$]$_2$ (0.050 g, 0.038 mmol), was dissolved in THF (5 mL) to create a red solution. In a separate vial, (4,4′-bipy){Ti(N[^{t}Bu]Ar)$_3$}$_2$ (0.102 g, 0.0382 mmol) was dissolved in THF (5 mL) to create a black solution. The black solution was added to the red solution dropwise, with stirring. Upon completion of the addition, the reaction mixture was a dark brown color. The reaction mixture was allowed to stir for one hour at which time all volatile materials were removed under reduced pressure to yield a brown oil. The oil was dissolved in Et_2O (3 mL) and *n*-hexane (15 mL) was added to the solution. After removing all volatile materials from the mixture under vacuum, an oily, brown solid was obtained. The solid was slurried in *n*-hexane (15 mL) and once again subjected to the removal of all volatile materials, yielding a light brown powder. The brown powder was slurried in *n*-hexane (10 mL) and the solids were isolated by filtration. The material was characterized as [(4,4′-bipy){Ti(N[^{t}Bu]Ar)$_3$}$_2$]-[B(C$_6$F$_5$)$_4$] by its color and by the fact that it was observed to be NMR silent (paramagnetic). Yield: 0.124 g, 0.0616 mmol, 81% (based on $C_{106}H_{116}BN_8F_{20}Ti_2$, 1988.62 g mol^{-1}).

3.9 Preparation of [Ti(N[^{t}Bu]Ar)$_3$][B(C$_6$F$_5$)$_4$]

Titanium trisanilide, Ti(N[^{t}Bu]Ar)$_3$ (0.500 g, 0.867 mmol), was dissolved in Et_2O (30 mL) to create a bright green solution. In a separate flask, the ferrocenium salt, Fc[B(C$_6$F$_5$)$_4$] (0.750 g, 0.867 mmol), was slurried in Et_2O (10 mL). The slurry was added dropwise, with stirring, to the Ti(N[^{t}Bu]Ar)$_3$ solution. Additional Et_2O (10 mL) was used to transfer the Fc[B(C$_6$F$_5$)$_4$] that remained behind in the original flask. During the course of the addition, the color of the reaction mixture turned from bright green to bright red-orange. The reaction mixture was allowed to stir for an additional 30 minutes and then were removed all volatile materials. The resulting sticky, red oil was dissolved in Et_2O (5 mL), *n*-hexane (30 mL) was added, and then from the new mixture were removed all volatile materials. This step was repeated, and the resulting orange powder was slurried in *n*-hexane (30 mL) before removing once again all volatile materials. It is essential to repeatedly triturate the material with *n*-hexane in order to remove all the coordinated solvent molecules. Finally, the orange powder was slurried in *n*-hexane (30 mL), collected by filtration using a frit, and washed with *n*-hexane until the washings became colorless. The orange filtrate was concentrated under vacuum and ferrocene (0.1284 g) was recovered (80% of expected). The orange powder in the frit was further kept under vacuum for 1 hour. Yield: 1.057 g, 0.842 mmol, 97% (based on $C_{60}H_{54}BN_3F_{20}Ti$, 1255.74 g mol^{-1}). Crystals suitable for X-ray diffraction were grown by dissolving [Ti(N[^{t}Bu]Ar)$_3$][B(C$_6$F$_5$)$_4$] (0.20 g) in *o*-difluorobenzene. The red solution was transferred to an NMR tube and *n*-hexane was layered on top. The tube was left undisturbed at room temperature for five days, during which time large, red, block-like crystals grew on the sides of the tube. Anal. Calcd: C 57.39; H 4.33; N 3.35. Found: C 57.13; H 4.61; N 3.07. ^{1}H NMR (pyridine-d_5, 20 °C, 400 MHz): δ = 6.99 (s, 3H, *H*Ar), 6.91 (s, 6H, *H*Ar), 2.31 (s, 18H, Ar–CH_3), 1.29 (s, 27H, C(CH_3)$_3$) ppm. ^{1}H NMR (THF-d_8, 20 °C, 400 MHz): δ = 7.13 (s, 3H, *H*Ar), 6.84 (s, 6H, *H*Ar), 2.40 (s, 18H, Ar–CH$_3$), 1.28 (s, 27H, C(CH$_3$)$_3$) ppm. ^{13}C NMR (pyridine-d_5, 20 °C, 125.7 MHz): δ = 149 (d, half of doublet hidden under pyridine-d_5 resonance, *C*–F), 142.5 (s, aryl *ipso*), 139.6 (s, *m*-Ar), 139.3 (d, J_{CF} = 246 Hz, *C*–F), 137.4 (d, J_{CF} = 232 Hz, *C*–F), 132.0 (s, *p*-Ar), 130.2 (s, *o*-Ar), 125.8 (m, *C*–F), 66.9 (s, N*C*(CH$_3$)$_3$), 30.7 (s, Ar*C*H$_3$), 21.6 (s, NC(*C*H$_3$)$_3$) ppm. ^{13}C NMR (THF-d_8, 20 °C, 125.7 MHz): δ = 149.3 (d, J_{CF} = 238 Hz, *C*–F), 144.4 (s, aryl *ipso*), 140.3 (d, J_{CF} = 246 Hz, *C*–F) 139.8 (s, *m*-Ar), 137.3 d, J_{CF} = 250 Hz, *C*–F), 131.6 (s, *p*-Ar), 129.4 (s, *o*-Ar), 125.5 (broad, *C*–F), 67.3 (s, N*C*(CH$_3$)$_3$), 30.9 (s, Ar*C*H$_3$), 21.4 (s, NC(*C*H$_3$)$_3$) ppm.

3.10 Crystallization of [(THF)Ti(N[^{t}Bu]Ar)$_3$][B(C$_6$F$_5$)$_4$]

[Ti(N[^{t}Bu]Ar)$_3$][B(C$_6$F$_5$)$_4$] (*ca.* 100 mg) was slurried in Et_2O (10 mL). THF was added (three to four drops) to completely dissolve the material. The orange solution was placed in the freezer at −35 °C. After two days, large, orange crystals were observed in the vial. The material continued to crystallize over the next two days, with large, orange crystals covering the base of the vial. A crystal was selected for the X-ray structure determination after about a week had passed. Attempts to grow crystals in a similar manner from toluene resulted in the material oiling out of solution. The material also did not crystallize out of concentrated THF solutions stored in the freezer.

3.11 Preparation of (^{n}BuO)Ti(N[^{t}Bu]Ar)$_3$

[Ti(N[^{t}Bu]Ar)$_3$][B(C$_6$F$_5$)$_4$] (0.192 g, 0.152 mmol) was dissolved in *o*-difluorobenzene (5 mL) to form a red solution, which was subsequently frozen solid in the dry box cold well. A solution of [Li][HBEt$_3$] (1.0 M in THF, 152 μL, 0.152 mmol) was added to the thawing red solution using a microsyringe. There was no immediate color change; however, the color of the reaction mixture gradually changed from red to orange to yellow upon warming to room temperature. The reaction mixture was allowed to stir for a total of one hour and then pumped down to dryness. The resulting yellow oil was triturated twice with *n*-hexane (10 mL) to give a yellow powder. This material was slurried in *n*-hexane and filtered to remove [Li][B(C$_6$F$_5$)$_4$]. The white solids present in the fritted funnel were washed with *n*-hexane until the washings became colorless. The yellow filtrate was pumped down to dryness to yield a yellow powder. Yield: 0.058 g, 0.089 mmol, 59%. Crystals suitable for X-ray diffraction were grown by first creating a slurry of the yellow powder in *n*-pentane and then adding Et_2O dropwise until all the material dissolved. The yellow solution so obtained was placed in the dry box freezer at −35 °C for five days, during which time yellow cubic crystals deposited. Anal. Calcd: C 73.92; H 9.78; N 6.47. Found: C 71.05; H 8.91; N 6.09. ^{1}H NMR (benzene-d_6, 20 °C, 400 MHz): δ 6.68 (s, 3H, *p*-Ar*H*), 5.83 (br s, 6H, *o*-Ar*H*), 4.53 (t, $^3J_{HH}$ = 7.6 Hz, 2H, OCH_2CH$_2$CH$_2$CH$_3$), 2.16 (s, 18H, Ar–CH_3), 1.83 (apparent pentet, *J* = 7.6 Hz, 2H,

Open Access Article. Published on 16 February 2015. Downloaded on 8/23/2022 12:27:23 PM.
This article is licensed under a Creative Commons Attribution 3.0 Unported Licence.

$OCH_2CH_2CH_2CH_3$), 1.41 (apparent sextet, J = 7.6 Hz, 2H, $OCH_2CH_2CH_2CH_3$), 1.10 (s, 27H, $C(CH_3)_3$), 0.99 (t, $^3J_{HH}$ = 7.6 Hz, $OCH_2CH_2CH_2CH_3$); ^{13}C NMR (benzene-d_6, 20 °C, 100.6 MHz): δ 152.7 (s, NAr *ipso*), 136.0 (s, *m*-Ar), 128.5 (s, *o*-Ar), 125.5 (s, *p*-Ar), 77.0 (s, $OCH_2CH_2CH_2CH_3$), 60.3 (s, $C(CH_3)_3$), 35.7 (s, $OCH_2CH_2CH_2CH_3$), 31.2 (s, $C(CH_3)_3$), 21.7 (s, Ar–CH_3), 19.3 (s, $OCH_2CH_2CH_2CH_3$), 14.3 ($OCH_2CH_2CH_2CH_3$).

3.12 X-Ray crystallography

Crystals were mounted in hydrocarbon oil on a nylon loop or a glass fiber. Low-temperature (100 K) data were collected on a Siemens Platform three-circle diffractometer coupled to a Bruker-AXS Smart Apex CCD detector with graphite-monochromated Mo-K_α radiation (λ = 0.71073) performing ψ- and ω-scans. A semi-empirical absorption correction was applied to the diffraction data using SADABS.[51] All structures were solved by direct or Patterson methods using SHELXS[52,53] and refined against F^2 on all data by full-matrix least squares with SHELXL-97.[53] All non-hydrogen atoms were refined anisotropically. All hydrogen atoms were included in the model at geometrically calculated positions and refined using a riding model. The isotropic displacement parameters of all hydrogen atoms were fixed to 1.2 times the U value of the atoms to which they are linked (1.5 times for methyl groups). In structures where disorders were present, the disorders were refined within SHELXL with the help of rigid bond restraints as well as similarity restraints on the anisotropic displacement parameters for neighboring atoms and on 1,2- and 1,3-distances throughout the disordered components. The relative occupancies of disordered components were refined freely within SHELXL.[54] The unit cell of $[(4,4'\text{-bipy})\{Ti(N[^tBu]Ar)_3\}_2]$-$[B(C_6F_5)_4]_2$ contains one *o*-difluorobenzene molecule residing atop the inversion center which has been treated as a diffuse contribution to the overall scattering without specific atom positions by SQUEEZE/PLATON.[55] Further details on all structures are provided in Tables S1 and S2.†

3.13 Electrochemistry

Electrochemical measurements were made using a BAS CV50W potentiostat with a platinum disk working electrode, platinum wire counter electrode, and a silver wire pseudoreference electrode. Potentials were internally referenced to the ferrocene/ferrocenium redox couple at 0 mV. Measurements were made under an atmosphere of purified nitrogen using THF solutions of $[N^nBu_4][B(C_6F_5)_4]$ (0.2 M), which was synthesized using modified literature methods.[56] The cyclic voltammograms of the complexes were collected at the sweep rates specified in the figure captions.

4 Conclusions

The exploration recounted herein, irrespective of initial motivation, led to an important outcome in the form of the synthesis, isolation, and thorough characterization of an exceedingly rare metal tris-amide cation, $\{Ti(N[^tBu]Ar)_3\}^+$, in a form that is unstabilized by coordination of donor solvent molecules. This accomplishment was made possible by the judicious choice of a robust counter-anion, namely the perfluorinated tetraphenylborate anion, $[B(C_6F_5)_4]^-$. The latter has been reported previously to permit isolation of extremely electrophilic cations, such as in the salt originally formulated as triethylsilyl perfluoro-tetraphenylborate, $[Et_3Si][B(C_6F_5)_4]$,[57,58] but recently shown actually to have the composition $[Et_3Si–H–SiEt_3][B(C_6F_5)_4]$,[59] and thus still able to serve as a source of triethylsilylium ion *via* release of an equivalent of triethylsilane. The latter silylium ion source has exhibited impressive stoichiometric reactivity that has spawned applications in catalysis.[60] The titanium tris-amide cation $\{Ti(N[^tBu]Ar)_3\}^+$ can now be explored in analogous fashion as a unique and powerful Lewis acid: based upon the observation that neutral $Ti(N[^tBu]Ar)_3$ readily abstracts a halogen atom from substrates including $ISiMe_3$, bromobenzene, and triphenyltin chloride to form $XTi(N[^tBu]Ar)_3$ (X = I, Br, or Cl),[5–7] the titanium(IV)–halogen bond energy in this system exceeds those found in the corresponding group 14 element–halogen compounds.

Acknowledgements

The authors are grateful to Syngenta for support and for helpful discussions with Dr David A. Jackson and Prof. Clark R. Landis. Nicholas Piro is thanked for his help in solving the structure of $(4,4'\text{-bipy})\{Ti(N[^tBu]Ar_3\}_2$ and Matthew Rankin is thanked for aiding with NMR data collection.

References

1 L. D. Durfee, P. E. Fanwick, I. P. Rothwell, K. Folting and J. C. Huffman, *J. Am. Chem. Soc.*, 1987, **109**, 4720–4722.
2 A. Mendiratta and C. C. Cummins, *Inorg. Chem.*, 2005, **44**, 7319–7321.
3 P. W. Wanandi, W. M. Davis, C. C. Cummins, M. A. Russell and D. E. Wilcox, *J. Am. Chem. Soc.*, 1995, **117**, 2110–2111.
4 (*a*) P. Girard, J. L. Namy and H. B. Kagan, *J. Am. Chem. Soc.*, 1980, **102**, 2693–2698; (*b*) A. Krief and A.-M. Laval, *Chem. Rev.*, 1999, **99**, 745–778.
5 T. Agapie, P. L. Diaconescu, D. J. Mindiola and C. C. Cummins, *Organometallics*, 2002, **21**, 1329–1340.
6 T. Agapie, P. L. Diaconescu and C. C. Cummins, *J. Am. Chem. Soc.*, 2002, **124**, 2412–2413.
7 B. M. Cossairt and C. C. Cummins, *New J. Chem.*, 2010, **34**, 1533–1536.
8 (*a*) K. J. Covert and P. T. Wolczanski, *Inorg. Chem.*, 1989, **28**, 4565–4567; (*b*) K. J. Covert, P. T. Wolczanski, S. A. Hill and P. J. Krusic, *Inorg. Chem.*, 1992, **31**, 66–78.
9 A. Mendiratta, J. S. Figueroa and C. C. Cummins, *Chem. Commun.*, 2005, 3403–3405.
10 E. Kim, A. L. Odom and C. C. Cummins, *Inorg. Chim. Acta*, 1998, **278**, 103–107.

 This journal is © The Royal Society of Chemistry 2015

Open Access Article. Published on 16 February 2015. Downloaded on 8/23/2022 12:27:23 PM.
This article is licensed under a Creative Commons Attribution 3.0 Unported Licence.

11 J. C. Peters, A. R. Johnson, A. L. Odom, P. W. Wanandi, W. M. Davis and C. C. Cummins, *J. Am. Chem. Soc.*, 1996, **118**, 10175–10188.
12 J. C. Peters, J.-P. F. Cherry, J. C. Thomas, L. Baraldo, D. J. Mindiola, W. M. Davis and C. C. Cummins, *J. Am. Chem. Soc.*, 1999, **121**, 10053–10067.
13 A. Lichtblau, H. D. Hausen, W. Schwarz and W. Kaim, *Inorg. Chem.*, 1993, **32**, 73–78.
14 S. Kraft, E. Hanuschek, R. Beckhaus, D. Haase and W. Saak, *Chem. – Eur. J.*, 2005, **11**, 969–978.
15 PLATON[55] was used to generate all ORTEP[61] diagrams in this work.
16 This Figure is based upon a model system that was geometry optimized using ADF 2006.01[62] using the LDA functional of Vosko, Wilk, and Nusair[63] together with the GGA functional known as OLYP[64] which is a combination of Handy and Cohen's OPTX functional[65] for exchange and Lee, Yang, and Parr's nonlocal correlation functional.[66] The zero-order regular approximation[67] (ZORA) was used for inclusion of relativistic effects. The basis sets were QZ4P for Ti and N, and TZ2P for C and H as supplied with ADF. Orbital contours were analyzed using the DGrid package[68] of Kohout.
17 D. E. Richardson and H. Taube, *Inorg. Chem.*, 1981, **20**, 1278–1285.
18 A. Bard and L. Faulkner, *Electrochemical Methods: Fundamentals and Applications*, Wiley, 2001.
19 M. B. Robin and P. Day, *Adv. Inorg. Chem. Radiochem.*, 1967, **10**, 247–466.
20 N. G. Connelly and W. E. Geiger, *Chem. Rev.*, 1996, **96**, 877–910.
21 A. Nafady, T. T. Chin and W. E. Geiger, *Organometallics*, 2006, **25**, 1654–1663.
22 T. R. O'Toole, J. N. Younathan, B. P. Sullivan and T. J. Meyer, *Inorg. Chem.*, 1989, **28**, 3923–3926.
23 C. Boisson, J. C. Berthet, M. Ephritikhine, M. Lance and M. Nierlich, *J. Organomet. Chem.*, 1997, **531**, 115–119.
24 I. Chávez, A. Alvarez-Carena, E. Molins, A. Roig, W. Maniukiewicz, A. Arancibia, V. Arancibia, H. Brand and J. Manuel Manríquez, *J. Organomet. Chem.*, 2000, **601**, 126–132.
25 K. B. P. Ruppa, N. Desmangles, S. Gambarotta, G. Yap and A. L. Rheingold, *Inorg. Chem.*, 1997, **36**, 1194–1197.
26 D. Reardon, I. Kovacs, K. B. P. Ruppa, K. Feghali, S. Gambarotta and J. Petersen, *Chem. – Eur. J.*, 1997, **3**, 1482–1488.
27 C. E. Laplaza, A. L. Odom, W. M. Davis, C. C. Cummins and J. D. Protasiewicz, *J. Am. Chem. Soc.*, 1995, **117**, 4999–5000.
28 C. E. Laplaza, M. J. A. Johnson, J. C. Peters, A. L. Odom, E. Kim, C. C. Cummins, G. N. George and I. J. Pickering, *J. Am. Chem. Soc.*, 1996, **118**, 8623–8638.
29 J.-P. F. Cherry, A. R. Johnson, L. M. Baraldo, Y.-C. Tsai, C. C. Cummins, S. V. Kryatov, E. V. Rybak-Akimova, K. B. Capps, C. D. Hoff, C. M. Haar and S. P. Nolan, *J. Am. Chem. Soc.*, 2001, **123**, 7271–7286.
30 C. Schädle, C. Meermann, K. W. Törnroos and R. Anwander, *Eur. J. Inorg. Chem.*, 2010, **2010**, 2841–2852.
31 R. A. Andersen, *Inorg. Chem.*, 1979, **18**, 1507–1509.
32 J. S. Ghotra, M. B. Hursthouse and A. J. Welch, *J. Chem. Soc., Chem. Commun.*, 1973, 669–670.
33 R. F. W. Bader, *Atoms in molecules: a quantum theory*, Clarendon Press, Oxford, New York, 1990.
34 The calculations used the M06 functional[69] and the def2-TZVPP basis set of Alrichs[70] as implemented in ORCA[71] (Default-Basis-4).
35 E. D. Glendening, C. R. Landis and F. Weinhold, *J. Comput. Chem.*, 2013, **34**, 1429–1437.
36 E. D. Glendening, C. R. Landis and F. Weinhold, *WIREs Comput. Mol. Sci.*, 2012, **2**, 1–42.
37 E. D. Glendening and F. Weinhold, *J. Comput. Chem.*, 1998, **19**, 593–609.
38 E. D. Glendening and F. Weinhold, *J. Comput. Chem.*, 1998, **19**, 610–627.
39 E. D. Glendening, J. K. Badenhoop and F. Weinhold, *J. Comput. Chem.*, 1998, **19**, 628–646.
40 The natural resonance theory (NRT) routine provided by NBO employs an alternative definition of valence as compared to the traditional one described by Sidgwick[72] and more recently by Parkin.[73] For example, NRT gives boron a natural valence of four for the boron atom in trigonal-planar BF_3 rather than a traditional valence of three due to equating "natural valence" to the total number of electron-pair bonds formed, rather than to the number of central-atom valence electrons used in bonding.
41 A. R. Johnson, P. W. Wanandi, C. C. Cummins and W. M. Davis, *Organometallics*, 1994, **13**, 2907–2909.
42 J. R. Galsworthy, M. L. H. Green, N. Maxted and M. Müller, *J. Chem. Soc., Dalton Trans.*, 1998, 387–392.
43 H. Aneetha, F. Basuli, J. Bollinger, J. C. Huffman and D. J. Mindiola, *Organometallics*, 2006, **25**, 2402–2404.
44 A. Shafir and J. Arnold, *J. Am. Chem. Soc.*, 2001, **123**, 9212–9213.
45 H. Nöth and M. Schmidt, *Organometallics*, 1995, **14**, 4601–4610.
46 K. Ma, W. E. Piers, Y. Gao and M. Parvez, *J. Am. Chem. Soc.*, 2004, **126**, 5668–5669.
47 Z. Y. Guo, P. K. Bradley and R. F. Jordan, *Organometallics*, 1992, **11**, 2690–2693.
48 W. J. Evans, T. A. Ulibarri, L. R. Chamberlain, J. W. Ziller and D. Alvarez, *Organometallics*, 1990, **9**, 2124–2130.
49 R. R. Schrock, L. G. Sturgeoff and P. R. Sharp, *Inorg. Chem.*, 1983, **22**, 2801–2806.
50 A. Massey and A. Park, *J. Organomet. Chem.*, 1964, **2**, 245–250.
51 G. M. Sheldrick, *SADABS*, Bruker AXS, Inc., 2005.
52 G. M. Sheldrick, *Acta Crystallogr., Sect. A: Fundam. Crystallogr.*, 1990, **46**, 467–473.
53 G. M. Sheldrick, *Acta Crystallogr., Sect. A: Fundam. Crystallogr.*, 2008, **64**, 112–122.
54 P. Müller, R. Herbst-Irmer, A. L. Spek, T. R. Schneider and M. R. Sawaya, *Crystal structure refinement: a crystallographers guide to SHELXL*, Oxford University Press, Oxford, New York, 2006.

Open Access Article. Published on 16 February 2015. Downloaded on 8/23/2022 12:27:23 PM.
This article is licensed under a Creative Commons Attribution 3.0 Unported Licence.

55 A. L. Spek, *J. Appl. Crystallogr.*, 2003, 7–13.
56 R. J. LeSuer, C. Buttolph and W. E. Geiger, *Anal. Chem.*, 2004, **76**, 6395–6401.
57 J. B. Lambert and S. Zhang, *J. Chem. Soc., Chem. Commun.*, 1993, 383–384.
58 J. B. Lambert, S. Zhang and S. M. Ciro, *Organometallics*, 1994, **13**, 2430–2443.
59 M. Nava and C. A. Reed, *Organometallics*, 2011, **30**, 4798–4800.
60 H. F. T. Klare and M. Oestreich, *Dalton Trans.*, 2010, **39**, 9176–9184.
61 M. N. Burnett and C. K. Johnson, ORTEP-III: Oak Ridge Thermal Ellipsoid Plot Program for Crystal Structure Illustrations, Oak Ridge National Laboratory Report ORNL-6895, 1996.
62 G. te Velde, F. M. Bickelhaupt, E. J. Baerends, C. F. Guerra, S. J. A. van Gisbergen, J. G. Snijders and T. Ziegler, *J. Comput. Chem.*, 2001, **22**, 931–967.
63 S. H. Vosko, L. Wilk and M. Nusair, *Can. J. Phys.*, 1980, **58**, 1200–1211.
64 J. Baker and P. Pulay, *J. Comput. Chem.*, 2003, **24**, 1184–1191.
65 W.-M. Hoe, A. J. Cohen and N. C. Handy, *Chem. Phys. Lett.*, 2001, **341**, 319–328.
66 C. Lee, W. Yang and R. G. Parr, *Phys. Rev. B: Condens. Matter*, 1988, **37**, 785–789.
67 (*a*) E. van Lenthe, E. J. Baerends and J. G. Snijders, *J. Chem. Phys.*, 1993, **99**, 4597–4610; (*b*) E. van Lenthe, E. J. Baerends and J. G. Snijders, *J. Chem. Phys.*, 1994, **101**, 9783–9792; (*c*) E. van Lenthe, A. Ehlers and E.-J. Baerends, *J. Chem. Phys.*, 1999, **110**, 8943–8953.
68 A. I. Baranov and M. Kohout, *J. Phys. Chem. Solids*, 2010, **71**, 1350–1356.
69 Y. Zhao and D. Truhlar, *Theor. Chem. Acc.*, 2008, **120**, 215–241.
70 A. Schäfer, H. Horn and R. Ahlrichs, *J. Chem. Phys.*, 1992, **97**, 2571–2577.
71 F. Neese, *WIREs Comput. Mol. Sci.*, 2012, **2**, 73–78.
72 N. V. Sidgwick, *The electronic theory of valency*, Clarendon Press, Oxford, 1927.
73 G. Parkin, *J. Chem. Educ.*, 2006, **83**, 791–799.

This journal is © The Royal Society of Chemistry 2015